Observation of the Decay Ξb- →pK-K-

Aaij, R.; Adeva, B.; Adinolfi, M.; Ajaltouni, Z.; Akar, S.; Albrecht, J.; Alessio, F.; Alexander, M.; Ali, S.; Alkhazov, G.; Alvarez Cartelle, P.; Alves, A. A.; Amato, S.; Amerio, S.; Amhis, Y.; An, L.; Anderlini, L.; Andreassi, G.; Andreotti, M.; Andrews, J. E.

DOI:
10.1103/PhysRevLett.118.071801

Observation of the Decay $\Xi_b^- \to pK^-K^-$

R. Aaij *et al.*[*]
(LHCb Collaboration)

(Received 8 December 2016; published 16 February 2017)

Decays of the Ξ_b^- and Ω_b^- baryons to the charmless final states $ph^-h'^-$, where $h^{(\prime)}$ denotes a kaon or pion, are searched for with the LHCb detector. The analysis is based on a sample of proton-proton collision data collected at center-of-mass energies $\sqrt{s} = 7$ and 8 TeV, corresponding to an integrated luminosity of 3 fb^{-1}. The decay $\Xi_b^- \to pK^-K^-$ is observed with a significance of 8.7 standard deviations, and evidence at the level of 3.4 standard deviations is found for the $\Xi_b^- \to pK^-\pi^-$ decay. Results are reported, relative to the $B^- \to K^+K^-K^-$ normalization channel, for the products of branching fractions and b-hadron production fractions. The branching fractions of $\Xi_b^- \to pK^-\pi^-$ and $\Xi_b^- \to p\pi^-\pi^-$ relative to $\Xi_b^- \to pK^-K^-$ decays are also measured.

DOI: 10.1103/PhysRevLett.118.071801

Decays of b hadrons to final states that do not contain charm quarks provide fertile ground for studies of CP violation, i.e., the breaking of symmetry under the combined charge conjugation and parity operations. Significant asymmetries have been observed between B and $\bar{B}$ partial widths in $\bar{B}^0 \to K^-\pi^+$ [1–4] and $\bar{B}_s^0 \to K^+\pi^-$ [3,4] decays. Even larger CP-violation effects have been observed in regions of the phase space of $B^- \to \pi^+\pi^-\pi^-$, $K^-\pi^+\pi^-$, $K^+K^-K^-$, and $K^+K^-\pi^-$ decays [5–7]. A number of theoretical approaches [8–18] have been proposed to determine whether the observed effects are consistent with being solely due to the nonzero phase in the quark mixing matrix [19,20] of the standard model, or whether additional sources of asymmetry are contributing.

Breaking of the symmetry between matter and antimatter has not yet been observed with a significance of more than 5 standard deviations (σ) in the properties of any baryon. Recently, however, the first evidence of CP violation in the b-baryon sector has been reported from an analysis of $\Lambda_b^0 \to p\pi^-\pi^+\pi^-$ decays [21]. Other CP-asymmetry parameters measured in Λ_b^0 baryon decays to $p\pi^-$, pK^- [3], $K_S^0 p\pi^-$ [22], ΛK^+K^-, and $\Lambda K^+\pi^-$ [23] final states are consistent with zero within the current experimental precision; these comprise the only charmless hadronic b-baryon decays that have been observed to date. It is therefore of great interest to search for additional charmless b-baryon decays that may be used in the future to investigate CP-violation effects.

[*]Full author list given at the end of the article.

In this Letter, the first search is presented for decays of Ξ_b^- and Ω_b^- baryons, with constituent quark contents of bsd and bss, to the charmless hadronic final states $ph^-h'^-$, where $h^{(\prime)}$ is a kaon or pion. The inclusion of charge-conjugate processes is implied throughout. Example decay diagrams for the $\Xi_b^- \to pK^-K^-$ mode are shown in Fig. 1. Interference between Cabibbo-suppressed tree and loop diagrams may lead to CP-violation effects. The $\Xi_b^- \to pK^-\pi^-$ and $\Omega_b^- \to pK^-K^-$ decays proceed by tree-level diagrams similar to that of Fig. 1 (left). Diagrams for $\Omega_b^- \to pK^-\pi^-$ and both Ξ_b^- and $\Omega_b^- \to p\pi^-\pi^-$ require additional weak interaction vertices. The rates of these decays are therefore expected to be further suppressed.

The analysis is based on a sample of proton-proton collision data, recorded by the LHCb experiment at center-of-mass energies $\sqrt{s} = 7$ and 8 TeV, corresponding to 3 fb^{-1} of integrated luminosity. Since the fragmentation fractions $f_{\Xi_b^-}$ and $f_{\Omega_b^-}$, which quantify the probabilities for a b quark to hadronize into these particular states, have not been determined, it is not possible to measure absolute branching fractions. Instead, the product of each branching fraction and the relevant fragmentation fraction is determined relative to the corresponding values for the topologically similar normalization channel $B^- \to K^+K^-K^-$

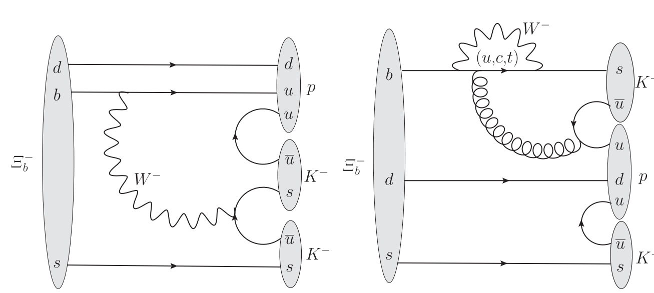

FIG. 1. Tree (left) and loop (right) diagrams for the $\Xi_b^- \to pK^-K^-$ decay channel.

(the B^- fragmentation fraction is denoted f_u). Once one significant signal yield is observed, it becomes possible to determine ratios of branching fractions for decays of the same baryon to different final states, thus canceling the dependence on the fragmentation fraction.

The LHCb detector [24,25] is a single-arm forward spectrometer covering the pseudorapidity range $2 < \eta < 5$, designed for the study of particles containing b or c quarks. The pseudorapidity is defined as $-\ln[\tan(\theta/2)]$ where θ is the polar angle relative to the beam axis. The detector elements that are particularly relevant to this analysis are a silicon-strip vertex detector surrounding the pp interaction region that allows b hadrons to be identified from their characteristically long flight distance, a tracking system that provides a measurement of the momentum p of charged particles, two ring-imaging Cherenkov detectors that enable different species of charged hadrons to be distinguished, and calorimeter and muon systems that provide information used for online event selection. Simulated data samples, produced with software described in Refs. [26–31], are used to evaluate the response of the detector to signal decays and to characterize the properties of certain types of background. These samples are generated separately for center-of-mass energies of 7 and 8 TeV, simulating the corresponding data-taking conditions, and combined in appropriate quantities.

On-line event selection is performed by a trigger [32] that consists of a hardware stage, based on information from the calorimeter and muon systems, followed by a software stage, which applies a full event reconstruction. At the hardware trigger stage, events are required to contain either a muon with high transverse momentum p_T or a particle that deposits high transverse energy in the calorimeters. For hadrons, the transverse energy threshold is typically 3.5 GeV. The software trigger for this analysis requires a two- or three-track secondary vertex with significant displacement from the primary pp interaction vertices (PVs). At least one charged particle must have p_T above a threshold of $1.7(1.6)\ \mathrm{GeV}/c$ in the $\sqrt{s} = 7(8)$ TeV data. This particle must also be inconsistent with originating from any PV as quantified through the difference in the vertex-fit χ^2 of a given PV reconstructed with and without the considered particle (χ^2_{IP}). A multivariate algorithm [33] is used for the identification of secondary vertices consistent with the decay of a b hadron.

The off-line selection of b-hadron candidates formed from three tracks is carried out with an initial prefiltering stage, a requirement on the output of a neural network [34], and particle identification criteria. To avoid potential bias, the properties of candidates with invariant masses in windows around the Ξ_b^- and Ω_b^- masses were not inspected until after the analysis procedures were finalized. The prefiltering includes requirements on the quality, p, p_T, and χ^2_{IP} of the tracks. Each b candidate must have a good quality vertex that is displaced from the closest PV (i.e., that with which it forms the smallest χ^2_{IP}), must satisfy p and p_T requirements, and must have reconstructed invariant mass loosely consistent with those of the b hadrons. A requirement is also imposed on the angle θ_{dir} between the b-candidate momentum vector and the line between the PV and the b-candidate decay vertex. In the off-line selection, trigger signals are associated with reconstructed particles. Selection requirements can therefore be made not only on which trigger caused the event to be recorded, but also on whether the decision was due to the signal candidate or other particles produced in the pp collision [32]. Only candidates from events with a hardware trigger caused by deposits of the signal in the calorimeter, or caused by other particles in the event, are retained. It is also required that the software trigger decision must have been caused by the signal candidate.

The inputs to the neural network for the final selection are the scalar sum of the p_T of all final-state tracks, the values of p_T and χ^2_{IP} for the highest p_T final-state track, the b-candidate $\cos(\theta_{\mathrm{dir}})$, vertex χ^2 and χ^2_{IP}, together with a combination of momentum information and θ_{dir} that characterizes how closely the momentum vector of the b candidate points back to the PV. The p_T asymmetry between the b candidate and other tracks within a circle, centered on the b candidate, with a radius $R = \sqrt{\delta\eta^2 + \delta\phi^2} < 1.5$ in the space of pseudorapidity and azimuthal angle ϕ (in radians) around the beam direction [35] is also used in the network. The distributions of these variables are consistent between simulated samples of signal decays and the $B^- \to K^+K^-K^-$ normalization channel, and between background-subtracted $B^- \to K^+K^-K^-$ data and simulation. The neural network input variables are also found to be not strongly correlated with either the b-candidate mass or the position in the phase space of the decay. The neural network is trained to distinguish signal from combinatorial background in the $B^- \to K^+K^-K^-$ channel, using a data-driven approach in which the two components are separated statistically using the *sPlot* method [36] with the b-candidate mass as the discriminating variable. The requirement on the neural network output is optimized using a figure of merit [37] intended to give the best chance to observe the signal decays. The same neural network output requirement is made for all signal final states, and has an efficiency of about 60%.

Using information from the ring-imaging Cherenkov detectors [38], criteria that identify uniquely the final-state tracks as either protons, pions, or kaons are imposed, ensuring that no candidate appears in more than one of the final states considered. For pions and kaons these criteria are optimized simultaneously with that on the neural network output, using the same figure of merit. The desire to reject possible background from $B^- \to K^+h^-h'^-$ in the signal modes justifies independent treatment of the proton identification requirement. In the simultaneous optimization, the efficiency is taken from control samples while the expected background level is extrapolated from sidebands in the b-candidate mass distribution. The combined efficiency of the particle identification requirements is about 30% for the pK^-K^-, 40% for the $pK^-\pi^-$, and 50% for the $p\pi^-\pi^-$ final state.

In order to ensure that any signal seen is due to charmless decays, candidates with pK^- invariant mass consistent with the $\Xi_b^- \to \Xi_c^0 h^- \to pK^-h^-$ or $\Xi_b^- \to \Xi_c^0 h^- \to p\pi^-h^-$ decay chain are vetoed. Similarly, candidates for the normalization channel with K^+K^- invariant mass consistent with the $B^- \to D^0 K^- \to K^+K^-K^-$ decay chain are removed. After all selection requirements are imposed, the fraction of selected events that contain more than one candidate is much less than 1%; all such candidates are retained.

The yields of the signal decays are obtained from a simultaneous unbinned extended maximum likelihood fit to the b-candidate mass distributions in the three $ph^-h'^-$ final states. This approach allows potential cross feed from one channel to another, due to particle misidentification, to be constrained according to the expected rates. The yield of the normalization channel is determined from a separate fit to the $K^+K^-K^-$ mass distribution.

Each signal component is modeled with the sum of two Crystal Ball (CB) functions [39] with shared parameters describing the core width and peak position and with non-Gaussian tails to both sides. The tail parameters and the relative normalization of the CB functions are determined from simulation. A scale factor relating the width in data to that in simulation is determined from the fit to the normalization channel. In the fit to the signal modes the peak positions are fixed to the known Ξ_b^- and Ω_b^- masses [40–42]; the only free parameters associated with the signal components are the yields.

Cross-feed backgrounds from other decays to $ph^-h'^-$ final states are also modeled with the sum of two CB functions, with all shape parameters fixed according to simulation but the width scaled in the same way as signal components. Cross-feed backgrounds from $B^- \to K^+h^-h'^-$ decays are modeled, in the mass interval of the fit, by exponential functions with shape fixed according to simulation. The yields of all cross-feed backgrounds are constrained according to expectations based on the yield in the correctly reconstructed channel and the (mis)identification probabilities determined from control samples.

In addition to signal and cross-feed backgrounds, components for partially reconstructed and combinatorial backgrounds are included in each final state. Partially reconstructed backgrounds arise due to b-hadron decays into final states similar to the signal, but with additional soft particles that are not reconstructed. Possible examples include $\Xi_b^- \to N^+h^-h'^- \to p\pi^0h^-h'^-$ and $\Xi_b^- \to pK^{*-}h^- \to pK^-\pi^0h^-$. Such decays are investigated with simulation and it is found that many of them have similar b-candidate mass distributions. The shapes of these backgrounds are therefore taken from $\Xi_b^- \to N^+h^-h'^- \to p\pi^0h^-h'^-$ simulation, with possible additional contributions considered as a source of systematic uncertainty. The shapes are modeled with an ARGUS function [43] convolved with a Gaussian function. The parameters of these functions are taken from simulation, except for the threshold of the ARGUS function, which is fixed to the known mass difference $m_{\Xi_b^-} - m_{\pi^0}$ [40,44]. The combinatorial background is modeled by an exponential function with the shape parameter shared between the three final states. Possible differences in the shape between the different final states are considered as a source of systematic uncertainty. The free parameters of the fit are the signal and background yields, and the combinatorial background shape parameter. The stability of the fit is confirmed using ensembles of pseudoexperiments with different values of signal yields.

The results of the fits are shown in Fig. 2. The significance of each of the signals is determined from the change in likelihood when the corresponding yield is fixed to zero, with relevant sources of systematic uncertainty taken into account. The signals for $\Xi_b^- \to pK^-K^-$ and $pK^-\pi^-$ decays are found to have a significance of 8.7σ and 3.4σ, respectively; each of the other signal modes has a significance less than 2σ. The relative branching fractions multiplied by fragmentation fractions are determined as

$$R_{ph^-h'^-} \equiv \frac{f_{\Xi_b}}{f_u}\frac{\mathcal{B}(\Xi_b^- \to ph^-h'^-)}{\mathcal{B}(B^- \to K^+K^-K^-)} = \frac{\mathcal{N}(\Xi_b^- \to ph^-h'^-)}{\mathcal{N}(B^- \to K^+K^-K^-)}\frac{\epsilon(B^- \to K^+K^-K^-)}{\epsilon(\Xi_b^- \to ph^-h'^-)}, \quad (1)$$

where the yields $\mathcal{N}$ are obtained from the fits. A similar expression is used for the Ω_b^- decay modes. The efficiencies ϵ are determined from simulation, weighted according to the most recent Ξ_b^- and Ω_b^- lifetime measurements [40–42], taking into account contributions from the detector geometry, reconstruction, and both on-line and off-line selection criteria. These are determined as a function of the position in phase space in each of the three-body final states. The phase space for each of the Ξ_b^- and Ω_b^- decays to $ph^-h'^-$ is five dimensional, but significant variations in efficiency occur only in the variables that describe the Dalitz plot. Simulation is used to evaluate each contribution to the efficiency except for the effect of the particle identification criteria, which is determined from data control samples weighted according to the expected kinematics of the signal tracks [38,45]. The description of reconstruction and selection efficiencies in the simulation has been validated with large control samples; the impact on the results of possible residual differences between data and simulation is negligible.

For the $\Xi_b^- \to pK^-K^-$, $\Xi_b^- \to pK^-\pi^-$, and $B^- \to K^+K^-K^-$ channels, efficiency corrections for each candidate are applied using the method of Ref. [46] to take the variation over the phase space into account. Using this procedure, the

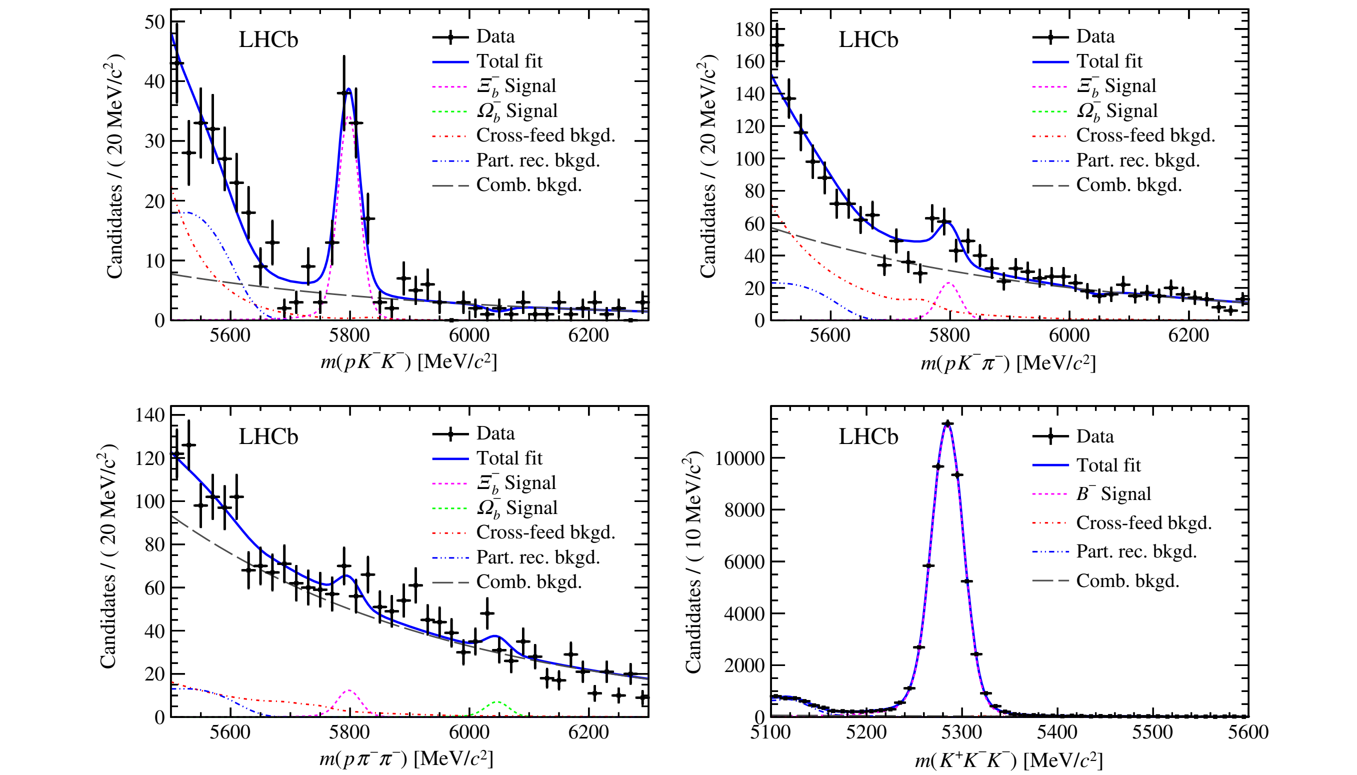

FIG. 2. Mass distributions for b-hadron candidates in the (top left) pK^-K^-, (top right) $pK^-\pi^-$, (bottom left) $p\pi^-\pi^-$, and (bottom right) $K^+K^-K^-$ final states. Results of the fits are shown with dark blue solid lines. Signals for Ξ_b^- and $B^-(\Omega_b^-)$ decays are shown with pink (light green) dashed lines, combinatorial backgrounds are shown with gray long-dashed lines, cross-feed backgrounds are shown with red dot-dashed lines, and partially reconstructed backgrounds are shown with dark blue double-dot-dashed lines.

efficiency-corrected and background-subtracted $m(pK^-)_{\rm min}$ distribution shown in Fig. 3 is obtained from $\Xi_b^- \to pK^-K^-$ candidates. Here, $m(pK^-)_{\rm min}$ indicates the smaller of the two $m(pK^-)$ values for each signal candidate, evaluated with the Ξ_b^- and the final-state particle masses fixed to their known values [40,44]. The distribution contains a clear peak from the $\Lambda(1520)$ resonance, a structure that is consistent with being a combination of the $\Lambda(1670)$ and $\Lambda(1690)$ states, and possible additional contributions at higher mass. Compared to the pK^- structures seen in the amplitude analysis of $\Lambda_b^0 \to J/\psi pK^-$ [47], the contributions from the broad $\Lambda(1600)$ and $\Lambda(1810)$ states appear to be smaller. A detailed amplitude analysis will be of interest when larger samples are available.

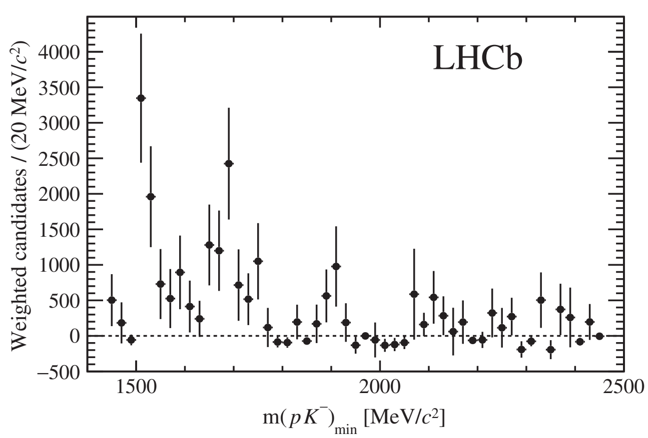

FIG. 3. Efficiency-corrected and background-subtracted [36] $m(pK^-)_{\rm min}$ distribution from $\Xi_b^- \to pK^-K^-$ candidates.

For channels without significant signal yields the efficiency averaged over phase space is used in Eq. (1). A corresponding systematic uncertainty is assigned from the variation of the efficiency over the phase space; this is the dominant source of systematic uncertainty for those channels. The quantities entering Eq. (1), and the results for $R_{ph^-h'^-}$, are reported in Table I. When the signal significance is less than 3σ, upper limits are set by integrating the likelihood after multiplying by a prior probability distribution that is uniform in the region of positive branching fraction.

The sources of systematic uncertainty arise from the fit model and the knowledge of the efficiency. The fit model is changed by varying the fixed parameters of the model, using alternative shapes for the components, and by including components that are omitted in the baseline fit. Intrinsic biases in the fitted yields are investigated with simulated pseudoexperiments, and are found to be negligible. Uncertainties in the efficiency arise due to the limited size of the simulation samples and possible residual differences between data and simulation in the trigger and

TABLE I. Fitted yields, efficiencies, and relative branching fractions multiplied by fragmentation fractions ($R_{ph^-h'^-}$). The two uncertainties quoted on $R_{ph^-h'^-}$ are statistical and systematic. Upper limits are quoted at 90% (95%) confidence level for modes with a signal significance less than 3σ. Uncertainties on the efficiencies are not given as only the relative uncertainties affect the branching fraction measurements.

Mode	Yield $\mathcal{N}$	Efficiency ϵ (%)	$R_{ph^-h'^-}(10^{-5})$
$\Xi_b^- \to pK^-K^-$	82.9 ± 10.4	0.398	$265 \pm 35 \pm 47$
$\Xi_b^- \to pK^-\pi^-$	59.6 ± 16.0	0.293	$259 \pm 64 \pm 49$
$\Xi_b^- \to p\pi^-\pi^-$	33.2 ± 17.9	0.573	$74 \pm 40 \pm 36 < 147$ (166)
$\Omega_b^- \to pK^-K^-$	-2.8 ± 2.5	0.375	$-9 \pm 9 \pm 6 < 18$ (22)
$\Omega_b^- \to pK^-\pi^-$	-7.6 ± 9.2	0.418	$-23 \pm 28 \pm 23 < 51$ (62)
$\Omega_b^- \to p\pi^-\pi^-$	20.1 ± 13.8	0.536	$48 \pm 33 \pm 28 < 109$ (124)
$B^- \to K^+K^-K^-$	$50\,490 \pm 250$	0.643	...

particle identification efficiencies [48]. Possible biases in the results due to the vetoes of charm hadrons are also accounted for. The efficiency depends on the signal decay-time distribution, and therefore the precision of the Ξ_b^- and Ω_b^- lifetime measurements [40–42] is a source of uncertainty. Similarly, the p_T distribution assumed for signal decays in the simulation affects the efficiency. Since the p_T spectra for Ξ_b^- and Ω_b^- baryons produced in LHC collisions have not been measured, the effect is estimated by weighting simulation to the background-subtracted [36] p_T distribution for $\Xi_b^- \to pK^-K^-$ decays obtained from the data. The difference in the average efficiency between the weighted and unweighted simulation is assigned as the associated systematic uncertainty. This is the dominant source of systematic uncertainty for the $\Xi_b^- \to pK^-K^-$ and $\Xi_b^- \to pK^-\pi^-$ modes.

The yield of $\Xi_b^- \to pK^-K^-$ decays is sufficient to use as normalization for the relative branching fractions of the other Ξ_b^- decays. The results are

$$\frac{\mathcal{B}(\Xi_b^- \to pK^-\pi^-)}{\mathcal{B}(\Xi_b^- \to pK^-K^-)} = 0.98 \pm 0.27(\mathrm{stat}) \pm 0.09(\mathrm{syst}),$$

$$\frac{\mathcal{B}(\Xi_b^- \to p\pi^-\pi^-)}{\mathcal{B}(\Xi_b^- \to pK^-K^-)} = 0.28 \pm 0.16(\mathrm{stat}) \pm 0.13(\mathrm{syst}) < 0.56(0.63),$$

where the upper limit is quoted at 90% (95%) confidence level. The same sources of systematic uncertainty as discussed above are considered. Since the effects due to the p_T distribution largely cancel, the dominant contributions are due to the trigger efficiency, fit model, and (for the $\Xi_b^- \to p\pi^-\pi^-$ mode) efficiency variation across the phase space.

In summary, a search for decays of Ξ_b^- and Ω_b^- baryons to $ph^-h'^-$ final states has been carried out with a sample of proton-proton collision data corresponding to an integrated luminosity of 3 fb^{-1}. The first observation of the $\Xi_b^- \to pK^-K^-$ decay, and first evidence for the $\Xi_b^- \to pK^-\pi^-$ decay, have been obtained; there is no significant signal for the other modes. This is the first observation of a Ξ_b decay to a charmless final state. These modes may be used in the future to search for CP asymmetries in the b-baryon sector.

We express our gratitude to our colleagues in the CERN accelerator departments for the excellent performance of the LHC. We thank the technical and administrative staff at the LHCb institutes. We acknowledge support from CERN and from the national agencies: CAPES, CNPq, FAPERJ, and FINEP (Brazil); NSFC (China); CNRS/IN2P3 (France); BMBF, DFG, and MPG (Germany); INFN (Italy); FOM and NWO (The Netherlands); MNiSW and NCN (Poland); MEN/IFA (Romania); MinES and FASO (Russia); MinECo (Spain); SNSF and SER (Switzerland); NASU (Ukraine); STFC (United Kingdom); and NSF (USA). We acknowledge the computing resources that are provided by CERN, IN2P3 (France); KIT and DESY (Germany); INFN (Italy); SURF (The Netherlands); PIC (Spain); GridPP (United Kingdom); RRCKI and Yandex LLC (Russia); CSCS (Switzerland); IFIN-HH (Romania); CBPF (Brazil); PL-GRID (Poland); and OSC (USA). We are indebted to the communities behind the multiple open source software packages on which we depend. Individual groups or members have received support from AvH Foundation (Germany); EPLANET, Marie Skłodowska-Curie Actions, and ERC (European Union); Conseil Général de Haute-Savoie, Labex ENIGMASS, and OCEVU, Région Auvergne (France); RFBR and Yandex LLC (Russia); GVA, XuntaGal, and GENCAT (Spain); Herchel Smith Fund, The Royal Society, Royal Commission for the Exhibition of 1851, and the Leverhulme Trust (United Kingdom).

[1] J. P. Lees *et al.* (*BABAR* Collaboration), Measurement of *CP* asymmetries and branching fractions in charmless two-body *B*-meson decays to pions and kaons, Phys. Rev. D **87**, 052009 (2013).

[2] Y.-T. Duh *et al.* (Belle Collaboration), Measurements of branching fractions and direct *CP* asymmetries for $B \to K\pi$,

$B \to \pi\pi$ and $B \to KK$ decays, Phys. Rev. D **87**, 031103 (2013).
[3] T. A. Aaltonen *et al.* (CDF Collaboration), Measurements of Direct CP-Violating Asymmetries in Charmless Decays of Bottom Baryons, Phys. Rev. Lett. **113**, 242001 (2014).
[4] R. Aaij *et al.* (LHCb Collaboration), First Observation of CP Violation in the Decays of B_s^0 Mesons, Phys. Rev. Lett. **110**, 221601 (2013).
[5] R. Aaij *et al.* (LHCb Collaboration), Measurement of CP Violation in the Phase Space of $B^\pm \to K^\pm\pi^+\pi^-$ and $B^\pm \to K^\pm K^+ K^-$ Decays, Phys. Rev. Lett. **111**, 101801 (2013).
[6] R. Aaij *et al.* (LHCb Collaboration), Measurement of CP Violation in the Phase Space of $B^\pm \to K^+K^-\pi^\pm$ and $B^\pm \to \pi^+\pi^-\pi^\pm$ Decays, Phys. Rev. Lett. **112**, 011801 (2014).
[7] R. Aaij *et al.* (LHCb Collaboration), Measurement of CP violation in the three-body phase space of charmless $B^\pm$ decays, Phys. Rev. D **90**, 112004 (2014).
[8] M. Gronau and J. L. Rosner, Implications for CP asymmetries of improved data on $B \to K^0\pi^0$, Phys. Lett. B **666**, 467 (2008).
[9] S. Baek, Cheng-Wei Chiang, Michael Gronau, David London, and Jonathan L. Rosner, Diagnostic for new physics in $B \to \pi K$ decays, Phys. Lett. B **678**, 97 (2009).
[10] M. Ciuchini, M. Pierini, and L. Silvestrini, New bounds on the CKM matrix from $B \to K\pi\pi$ Dalitz plot analyses, Phys. Rev. D **74**, 051301 (2006).
[11] M. Ciuchini, M. Pierini, and L. Silvestrini, Hunting the CKM weak phase with time-integrated Dalitz analyses of $B_s^0 \to KK\pi$ and $B_s^0 \to K\pi\pi$ decays, Phys. Lett. B **645**, 201 (2007).
[12] M. Gronau, D. Pirjol, A. Soni, and J. Zupan, Improved method for CKM constraints in charmless three-body B and B_s^0 decays, Phys. Rev. D **75**, 014002 (2007).
[13] M. Gronau, D. Pirjol, A. Soni, and J. Zupan, Constraint on $\bar\rho, \bar\eta$ from $B \to K^*\pi$, Phys. Rev. D **77**, 057504 (2008).
[14] I. Bediaga, G. Guerrer, and J. M. de Miranda, Extracting the quark mixing phase γ from $B^\pm \to K^\pm\pi^+\pi^-$, $B^0 \to K_S^0\pi^+\pi^-$, and $\bar B^0 \to K_S^0\pi^+\pi^-$, Phys. Rev. D **76**, 073011 (2007).
[15] M. Gronau, D. Pirjol, and J. Zupan, CP asymmetries in $B \to K\pi, K^*\pi, \rho K$ decays, Phys. Rev. D **81**, 094011 (2010).
[16] M. Gronau, D. Pirjol, and J. L. Rosner, Calculating phases between $B \to K^*\pi$ amplitudes, Phys. Rev. D **81**, 094026 (2010).
[17] M. Imbeault, N. Rey-Le Lorier, and D. London, Measuring γ in $B \to K\pi\pi$ decays, Phys. Rev. D **84**, 034041 (2011).
[18] B. Bhattacharya and D. London, Using U-spin to extract γ from charmless $B \to PPP$ decays, J. High Energy Phys. 04 (2015) 154.
[19] N. Cabibbo, Unitary Symmetry and Leptonic Decays, Phys. Rev. Lett. **10**, 531 (1963).
[20] M. Kobayashi and T. Maskawa, CP violation in the renormalizable theory of weak interaction, Prog. Theor. Phys. **49**, 652 (1973).
[21] R. Aaij *et al.* (LHCb Collaboration), Probing matter-antimatter asymmetries in beauty baryon decays, Nat. Phys., doi:10.1038/nphys4021 (2017).
[22] R. Aaij *et al.* (LHCb Collaboration), Searches for Λ_b^0 and Ξ_b^0 decays to $K_S^0 p\pi^-$ and $K_S^0 pK^-$ final states with first observation of the $\Lambda_b^0 \to K_S^0 p\pi^-$ decay, J. High Energy Phys. 04 (2014) 087.
[23] R. Aaij *et al.* (LHCb Collaboration), Observations of $\Lambda_b^0 \to \Lambda K^+\pi^-$ and $\Lambda_b^0 \to \Lambda K^+K^-$ decays and searches for other Λ_b^0 and Ξ_b^0 decays to Λh^+h^- final states, J. High Energy Phys. 05 (2016) 081.
[24] A. A. Alves Jr. *et al.* (LHCb Collaboration), The LHCb detector at the LHC, J. Instrum. **3**, S08005 (2008).
[25] R. Aaij *et al.* (LHCb Collaboration), LHCb detector performance, Int. J. Mod. Phys. A **30**, 1530022 (2015).
[26] T. Sjöstrand, S. Mrenna, and P. Skands, PYTHIA 6.4 physics and manual, J. High Energy Phys. 05 (2006) 026; T. Sjöstrand, S. Mrenna, and P. Skands, A brief introduction to PYTHIA 8.1, Comput. Phys. Commun. **178**, 852 (2008).
[27] I. Belyaev *et al.*, Handling of the generation of primary events in Gauss, the LHCb simulation framework, J. Phys. Conf. Ser. **331**, 032047 (2011).
[28] D. J. Lange, The EvtGen particle decay simulation package, Nucl. Instrum. Methods Phys. Res., Sect. A **462**, 152 (2001).
[29] P. Golonka and Z. Was, PHOTOS Monte Carlo: A precision tool for QED corrections in Z and W decays, Eur. Phys. J. C **45**, 97 (2006).
[30] J. Allison *et al.* (Geant4 Collaboration), Geant4 developments and applications, IEEE Trans. Nucl. Sci. **53**, 270 (2006); S. Agostinelli *et al.* (Geant4 Collaboration), Geant4: A simulation toolkit, Nucl. Instrum. Methods Phys. Res., Sect. A **506**, 250 (2003).
[31] M. Clemencic, G. Corti, S. Easo, C. R. Jones, S. Miglioranzi, M Pappagallo, and P Robbe, The LHCb simulation application, Gauss: Design, evolution and experience, J. Phys. Conf. Ser. **331**, 032023 (2011).
[32] R. Aaij *et al.*, The LHCb trigger and its performance in 2011, J. Instrum. **8**, P04022 (2013).
[33] V. V. Gligorov and M. Williams, Efficient, reliable and fast high-level triggering using a bonsai boosted decision tree, J. Instrum. **8**, P02013 (2013).
[34] M. Feindt and U. Kerzel, The NeuroBayes neural network package, Nucl. Instrum. Methods Phys. Res., Sect. A **559**, 190 (2006).
[35] R. Aaij *et al.* (LHCb Collaboration), Observation of CP violation in $B^\pm \to DK^\pm$ decays, Phys. Lett. B **712**, 203 (2012); Erratum, Phys. Lett. B **713**, 351(E) (2012).
[36] M. Pivk and F. R. Le Diberder, sPlot: A statistical tool to unfold data distributions, Nucl. Instrum. Methods Phys. Res., Sect. A **555**, 356 (2005).
[37] G. Punzi, in *Statistical Problems in Particle Physics, Astrophysics, and Cosmology*, edited by L. Lyons, R. Mount, and R. Reitmeyer (2003), p. 79; eConf **C030908** (2003) MODT002.
[38] M. Adinolfi *et al.*, Performance of the LHCb RICH detector at the LHC, Eur. Phys. J. C **73**, 2431 (2013).
[39] T. Skwarnicki, Ph. D. thesis, Institute of Nuclear Physics, Krakow, 1986 [DESY-F31-86-02].
[40] R. Aaij *et al.* (LHCb Collaboration), Precision Measurement of the Mass and Lifetime of the Ξ_b^- Baryon, Phys. Rev. Lett. **113**, 242002 (2014).

[41] R. Aaij *et al.* (LHCb Collaboration), Measurements of the mass and lifetime of the Ω_b^- baryon, Phys. Rev. D **93**, 092007 (2016).

[42] Y. Amhis *et al.* (Heavy Flavor Averaging Group), Averages of b-hadron, c-hadron, and τ-lepton properties as of summer 2014, arXiv:1412.7515. Updated results and plots are available at http://www.slac.stanford.edu/xorg/hfag/.

[43] H. Albrecht *et al.* (ARGUS Collaboration), Search for hadronic $b \to u$ decays, Phys. Lett. B **241**, 278 (1990).

[44] K. A. Olive *et al.* (Particle Data Group), Review of particle physics, Chin. Phys. C **38**, 090001 (2014). See also the 2015 update.

[45] L. Anderlini *et al.*, The PIDCalib package, Report No. LHCb-PUB-2016-021.

[46] R. Aaij *et al.* (LHCb Collaboration), Observation of $B^0 \to \bar{D}^0 K^+ K^-$ and Evidence for $B_s^0 \to \bar{D}^0 K^+ K^-$, Phys. Rev. Lett. **109**, 131801 (2012).

[47] R. Aaij *et al.* (LHCb Collaboration), Observation of $J/\psi p$ Resonances Consistent with Pentaquark States in $\Lambda_b^0 \to J/\psi p K^-$ Decays, Phys. Rev. Lett. **115**, 072001 (2015).

[48] R. Aaij *et al.* (LHCb Collaboration), Dalitz plot analysis of $B_s^0 \to \bar{D}^0 K^- \pi^+$ decays, Phys. Rev. D **90**, 072003 (2014).

R. Aaij,[40] B. Adeva,[39] M. Adinolfi,[48] Z. Ajaltouni,[5] S. Akar,[59] J. Albrecht,[10] F. Alessio,[40] M. Alexander,[53] S. Ali,[43] G. Alkhazov,[31] P. Alvarez Cartelle,[55] A. A. Alves Jr.,[59] S. Amato,[2] S. Amerio,[23] Y. Amhis,[7] L. An,[3] L. Anderlini,[18] G. Andreassi,[41] M. Andreotti,[17,a] J. E. Andrews,[60] R. B. Appleby,[56] F. Archilli,[43] P. d'Argent,[12] J. Arnau Romeu,[6] A. Artamonov,[37] M. Artuso,[61] E. Aslanides,[6] G. Auriemma,[26] M. Baalouch,[5] I. Babuschkin,[56] S. Bachmann,[12] J. J. Back,[50] A. Badalov,[38] C. Baesso,[62] S. Baker,[55] V. Balagura,[7,b] W. Baldini,[17] R. J. Barlow,[56] C. Barschel,[40] S. Barsuk,[7] W. Barter,[40] M. Baszczyk,[27] V. Batozskaya,[29] B. Batsukh,[61] V. Battista,[41] A. Bay,[41] L. Beaucourt,[4] J. Beddow,[53] F. Bedeschi,[24] I. Bediaga,[1] L. J. Bel,[43] V. Bellee,[41] N. Belloli,[21,c] K. Belous,[37] I. Belyaev,[32] E. Ben-Haim,[8] G. Bencivenni,[19] S. Benson,[43] A. Berezhnoy,[33] R. Bernet,[42] A. Bertolin,[23] C. Betancourt,[42] F. Betti,[15] M.-O. Bettler,[40] M. van Beuzekom,[43] Ia. Bezshyiko,[42] S. Bifani,[47] P. Billoir,[8] T. Bird,[56] A. Birnkraut,[10] A. Bitadze,[56] A. Bizzeti,[18,d] T. Blake,[50] F. Blanc,[41] J. Blouw,[11] S. Blusk,[61] V. Bocci,[26] T. Boettcher,[58] A. Bondar,[36,e] N. Bondar,[31,40] W. Bonivento,[16] I. Bordyuzhin,[32] A. Borgheresi,[21,c] S. Borghi,[56] M. Borisyak,[35] M. Borsato,[39] F. Bossu,[7] M. Boubdir,[9] T. J. V. Bowcock,[54] E. Bowen,[42] C. Bozzi,[17,40] S. Braun,[12] M. Britsch,[12] T. Britton,[61] J. Brodzicka,[56] E. Buchanan,[48] C. Burr,[56] A. Bursche,[2] J. Buytaert,[40] S. Cadeddu,[16] R. Calabrese,[17,a] M. Calvi,[21,c] M. Calvo Gomez,[38,f] A. Camboni,[38] P. Campana,[19] D. H. Campora Perez,[40] L. Capriotti,[56] A. Carbone,[15,g] G. Carboni,[25,h] R. Cardinale,[20,i] A. Cardini,[16] P. Carniti,[21,c] L. Carson,[52] K. Carvalho Akiba,[2] G. Casse,[54] L. Cassina,[21,c] L. Castillo Garcia,[41] M. Cattaneo,[40] G. Cavallero,[20] R. Cenci,[24,j] D. Chamont,[7] M. Charles,[8] Ph. Charpentier,[40] G. Chatzikonstantinidis,[47] M. Chefdeville,[4] S. Chen,[56] S.-F. Cheung,[57] V. Chobanova,[39] M. Chrzaszcz,[42,27] X. Cid Vidal,[39] G. Ciezarek,[43] P. E. L. Clarke,[52] M. Clemencic,[40] H. V. Cliff,[49] J. Closier,[40] V. Coco,[59] J. Cogan,[6] E. Cogneras,[5] V. Cogoni,[16,40,k] L. Cojocariu,[30] G. Collazuol,[23,l] P. Collins,[40] A. Comerma-Montells,[12] A. Contu,[40] A. Cook,[48] G. Coombs,[40] S. Coquereau,[38] G. Corti,[40] M. Corvo,[17,a] C. M. Costa Sobral,[50] B. Couturier,[40] G. A. Cowan,[52] D. C. Craik,[52] A. Crocombe,[50] M. Cruz Torres,[62] S. Cunliffe,[55] R. Currie,[55] C. D'Ambrosio,[40] F. Da Cunha Marinho,[2] E. Dall'Occo,[43] J. Dalseno,[48] P. N. Y. David,[43] A. Davis,[3] K. De Bruyn,[6] S. De Capua,[56] M. De Cian,[12] J. M. De Miranda,[1] L. De Paula,[2] M. De Serio,[14,m] P. De Simone,[19] C.-T. Dean,[53] D. Decamp,[4] M. Deckenhoff,[10] L. Del Buono,[8] M. Demmer,[10] A. Dendek,[28] D. Derkach,[35] O. Deschamps,[5] F. Dettori,[40] B. Dey,[22] A. Di Canto,[40] H. Dijkstra,[40] F. Dordei,[40] M. Dorigo,[41] A. Dosil Suárez,[39] A. Dovbnya,[45] K. Dreimanis,[54] L. Dufour,[43] G. Dujany,[56] K. Dungs,[40] P. Durante,[40] R. Dzhelyadin,[37] A. Dziurda,[40] A. Dzyuba,[31] N. Déléage,[4] S. Easo,[51] M. Ebert,[52] U. Egede,[55] V. Egorychev,[32] S. Eidelman,[36,e] S. Eisenhardt,[52] U. Eitschberger,[10] R. Ekelhof,[10] L. Eklund,[53] S. Ely,[61] S. Esen,[12] H. M. Evans,[49] T. Evans,[57] A. Falabella,[15] N. Farley,[47] S. Farry,[54] R. Fay,[54] D. Fazzini,[21,c] D. Ferguson,[52] A. Fernandez Prieto,[39] F. Ferrari,[15,40] F. Ferreira Rodrigues,[2] M. Ferro-Luzzi,[40] S. Filippov,[34] R. A. Fini,[14] M. Fiore,[17,a] M. Fiorini,[17,a] M. Firlej,[28] C. Fitzpatrick,[41] T. Fiutowski,[28] F. Fleuret,[7,n] K. Fohl,[40] M. Fontana,[16,40] F. Fontanelli,[20,i] D. C. Forshaw,[61] R. Forty,[40] V. Franco Lima,[54] M. Frank,[40] C. Frei,[40] J. Fu,[22,o] W. Funk,[40] E. Furfaro,[25,h] C. Färber,[40] A. Gallas Torreira,[39] D. Galli,[15,g] S. Gallorini,[23] S. Gambetta,[52] M. Gandelman,[2] P. Gandini,[57] Y. Gao,[3] L. M. Garcia Martin,[69] J. García Pardiñas,[39] J. Garra Tico,[49] L. Garrido,[38] P. J. Garsed,[49] D. Gascon,[38] C. Gaspar,[40] L. Gavardi,[10] G. Gazzoni,[5] D. Gerick,[12] E. Gersabeck,[12] M. Gersabeck,[56] T. Gershon,[50] Ph. Ghez,[4] S. Gianì,[41] V. Gibson,[49] O. G. Girard,[41] L. Giubega,[30] K. Gizdov,[52] V. V. Gligorov,[8] D. Golubkov,[32] A. Golutvin,[55,40] A. Gomes,[1,p] I. V. Gorelov,[33] C. Gotti,[21,c] R. Graciani Diaz,[38] L. A. Granado Cardoso,[40] E. Graugés,[38] E. Graverini,[42] G. Graziani,[18] A. Grecu,[30] P. Griffith,[47] L. Grillo,[21,40,c] B. R. Gruberg Cazon,[57] O. Grünberg,[67]

E. Gushchin,[34] Yu. Guz,[37] T. Gys,[40] C. Göbel,[62] T. Hadavizadeh,[57] C. Hadjivasiliou,[5] G. Haefeli,[41] C. Haen,[40] S. C. Haines,[49] S. Hall,[55] B. Hamilton,[60] X. Han,[12] S. Hansmann-Menzemer,[12] N. Harnew,[57] S. T. Harnew,[48] J. Harrison,[56] M. Hatch,[40] J. He,[63] T. Head,[41] A. Heister,[9] K. Hennessy,[54] P. Henrard,[5] L. Henry,[8] E. van Herwijnen,[40] M. Heß,[67] A. Hicheur,[2] D. Hill,[57] C. Hombach,[56] H. Hopchev,[41] W. Hulsbergen,[43] T. Humair,[55] M. Hushchyn,[35] D. Hutchcroft,[54] M. Idzik,[28] P. Ilten,[58] R. Jacobsson,[40] A. Jaeger,[12] J. Jalocha,[57] E. Jans,[43] A. Jawahery,[60] F. Jiang,[3] M. John,[57] D. Johnson,[40] C. R. Jones,[49] C. Joram,[40] B. Jost,[40] N. Jurik,[57] S. Kandybei,[45] M. Karacson,[40] J. M. Kariuki,[48] S. Karodia,[53] M. Kecke,[12] M. Kelsey,[61] M. Kenzie,[49] T. Ketel,[44] E. Khairullin,[35] B. Khanji,[12] C. Khurewathanakul,[41] T. Kirn,[9] S. Klaver,[56] K. Klimaszewski,[29] S. Koliiev,[46] M. Kolpin,[12] I. Komarov,[41] R. F. Koopman,[44] P. Koppenburg,[43] A. Kosmyntseva,[32] A. Kozachuk,[33] M. Kozeiha,[5] L. Kravchuk,[34] K. Kreplin,[12] M. Kreps,[50] P. Krokovny,[36,e] F. Kruse,[10] W. Krzemien,[29] W. Kucewicz,[27,q] M. Kucharczyk,[27] V. Kudryavtsev,[36,e] A. K. Kuonen,[41] K. Kurek,[29] T. Kvaratskheliya,[32,40] D. Lacarrere,[40] G. Lafferty,[56] A. Lai,[16] G. Lanfranchi,[19] C. Langenbruch,[9] T. Latham,[50] C. Lazzeroni,[47] R. Le Gac,[6] J. van Leerdam,[43] A. Leflat,[33,40] J. Lefrançois,[7] R. Lefèvre,[5] F. Lemaitre,[40] E. Lemos Cid,[39] O. Leroy,[6] T. Lesiak,[27] B. Leverington,[12] T. Li,[3] Y. Li,[7] T. Likhomanenko,[35,68] R. Lindner,[40] C. Linn,[40] F. Lionetto,[42] X. Liu,[3] D. Loh,[50] I. Longstaff,[53] J. H. Lopes,[2] D. Lucchesi,[23,l] M. Lucio Martinez,[39] H. Luo,[52] A. Lupato,[23] E. Luppi,[17,a] O. Lupton,[40] A. Lusiani,[24] X. Lyu,[63] F. Machefert,[7] F. Maciuc,[30] O. Maev,[31] K. Maguire,[56] S. Malde,[57] A. Malinin,[68] T. Maltsev,[36] G. Manca,[16,k] G. Mancinelli,[6] P. Manning,[61] J. Maratas,[5,r] J. F. Marchand,[4] U. Marconi,[15] C. Marin Benito,[38] M. Marinangeli,[41] P. Marino,[24,j] J. Marks,[12] G. Martellotti,[26] M. Martin,[6] M. Martinelli,[41] D. Martinez Santos,[39] F. Martinez Vidal,[69] D. Martins Tostes,[2] L. M. Massacrier,[7] A. Massafferri,[1] R. Matev,[40] A. Mathad,[50] Z. Mathe,[40] C. Matteuzzi,[21] A. Mauri,[42] E. Maurice,[7,n] B. Maurin,[41] A. Mazurov,[47] M. McCann,[55,40] A. McNab,[56] R. McNulty,[13] B. Meadows,[59] F. Meier,[10] M. Meissner,[12] D. Melnychuk,[29] M. Merk,[43] A. Merli,[22,o] E. Michielin,[23] D. A. Milanes,[66] M.-N. Minard,[4] D. S. Mitzel,[12] A. Mogini,[8] J. Molina Rodriguez,[1] I. A. Monroy,[66] S. Monteil,[5] M. Morandin,[23] P. Morawski,[28] A. Mordà,[6] M. J. Morello,[24,j] O. Morgunova,[68] J. Moron,[28] A. B. Morris,[52] R. Mountain,[61] F. Muheim,[52] M. Mulder,[43] M. Mussini,[15] D. Müller,[56] J. Müller,[10] K. Müller,[42] V. Müller,[10] P. Naik,[48] T. Nakada,[41] R. Nandakumar,[51] A. Nandi,[57] I. Nasteva,[2] M. Needham,[52] N. Neri,[22] S. Neubert,[12] N. Neufeld,[40] M. Neuner,[12] T. D. Nguyen,[41] C. Nguyen-Mau,[41,s] S. Nieswand,[9] R. Niet,[10] N. Nikitin,[33] T. Nikodem,[12] A. Nogay,[68] A. Novoselov,[37] D. P. O'Hanlon,[50] A. Oblakowska-Mucha,[28] V. Obraztsov,[37] S. Ogilvy,[19] R. Oldeman,[16,k] C. J. G. Onderwater,[70] J. M. Otalora Goicochea,[2] A. Otto,[40] P. Owen,[42] A. Oyanguren,[69] P. R. Pais,[41] A. Palano,[14,m] F. Palombo,[22,o] M. Palutan,[19] A. Papanestis,[51] M. Pappagallo,[14,m] L. L. Pappalardo,[17,a] W. Parker,[60] C. Parkes,[56] G. Passaleva,[18] A. Pastore,[14,m] G. D. Patel,[54] M. Patel,[55] C. Patrignani,[15,g] A. Pearce,[40] A. Pellegrino,[43] G. Penso,[26] M. Pepe Altarelli,[40] S. Perazzini,[40] P. Perret,[5] L. Pescatore,[47] K. Petridis,[48] A. Petrolini,[20,i] A. Petrov,[68] M. Petruzzo,[22,o] E. Picatoste Olloqui,[38] B. Pietrzyk,[4] M. Pikies,[27] D. Pinci,[26] A. Pistone,[20] A. Piucci,[12] V. Placinta,[30] S. Playfer,[52] M. Plo Casasus,[39] T. Poikela,[40] F. Polci,[8] A. Poluektov,[50,36] I. Polyakov,[61] E. Polycarpo,[2] G. J. Pomery,[48] A. Popov,[37] D. Popov,[11,40] B. Popovici,[30] S. Poslavskii,[37] C. Potterat,[2] E. Price,[48] J. D. Price,[54] J. Prisciandaro,[39,40] A. Pritchard,[54] C. Prouve,[48] V. Pugatch,[46] A. Puig Navarro,[42] G. Punzi,[24,t] W. Qian,[50] R. Quagliani,[7,48] B. Rachwal,[27] J. H. Rademacker,[48] M. Rama,[24] M. Ramos Pernas,[39] M. S. Rangel,[2] I. Raniuk,[45] F. Ratnikov,[35] G. Raven,[44] F. Redi,[55] S. Reichert,[10] A. C. dos Reis,[1] C. Remon Alepuz,[69] V. Renaudin,[7] S. Ricciardi,[51] S. Richards,[48] M. Rihl,[40] K. Rinnert,[54] V. Rives Molina,[38] P. Robbe,[7,40] A. B. Rodrigues,[1] E. Rodrigues,[59] J. A. Rodriguez Lopez,[66] P. Rodriguez Perez,[56] A. Rogozhnikov,[35] S. Roiser,[40] A. Rollings,[57] V. Romanovskiy,[37] A. Romero Vidal,[39] J. W. Ronayne,[13] M. Rotondo,[19] M. S. Rudolph,[61] T. Ruf,[40] P. Ruiz Valls,[69] J. J. Saborido Silva,[39] E. Sadykhov,[32] N. Sagidova,[31] B. Saitta,[16,k] V. Salustino Guimaraes,[1] C. Sanchez Mayordomo,[69] B. Sanmartin Sedes,[39] R. Santacesaria,[26] C. Santamarina Rios,[39] M. Santimaria,[19] E. Santovetti,[25,h] A. Sarti,[19,u] C. Satriano,[26,v] A. Satta,[25] D. M. Saunders,[48] D. Savrina,[32,33] S. Schael,[9] M. Schellenberg,[10] M. Schiller,[53] H. Schindler,[40] M. Schlupp,[10] M. Schmelling,[11] T. Schmelzer,[10] B. Schmidt,[40] O. Schneider,[41] A. Schopper,[40] K. Schubert,[10] M. Schubiger,[41] M.-H. Schune,[7] R. Schwemmer,[40] B. Sciascia,[19] A. Sciubba,[26,u] A. Semennikov,[32] A. Sergi,[47] N. Serra,[42] J. Serrano,[6] L. Sestini,[23] P. Seyfert,[21] M. Shapkin,[37] I. Shapoval,[45] Y. Shcheglov,[31] T. Shears,[54] L. Shekhtman,[36,e] V. Shevchenko,[68] B. G. Siddi,[17,40] R. Silva Coutinho,[42] L. Silva de Oliveira,[2] G. Simi,[23,l] S. Simone,[14,m] M. Sirendi,[49] N. Skidmore,[48] T. Skwarnicki,[61] E. Smith,[55] I. T. Smith,[52] J. Smith,[49] M. Smith,[55] H. Snoek,[43] l. Soares Lavra,[1] M. D. Sokoloff,[59] F. J. P. Soler,[53] B. Souza De Paula,[2] B. Spaan,[10] P. Spradlin,[53] S. Sridharan,[40] F. Stagni,[40] M. Stahl,[12] S. Stahl,[40] P. Stefko,[41] S. Stefkova,[55] O. Steinkamp,[42] S. Stemmle,[12] O. Stenyakin,[37] H. Stevens,[10] S. Stevenson,[57] S. Stoica,[30] S. Stone,[61] B. Storaci,[42] S. Stracka,[24,t] M. Straticiuc,[30] U. Straumann,[42] L. Sun,[64] W. Sutcliffe,[55] K. Swientek,[28] V. Syropoulos,[44] M. Szczekowski,[29]

T. Szumlak,[28] S. T'Jampens,[4] A. Tayduganov,[6] T. Tekampe,[10] G. Tellarini,[17,a] F. Teubert,[40] E. Thomas,[40] J. van Tilburg,[43] M. J. Tilley,[55] V. Tisserand,[4] M. Tobin,[41] S. Tolk,[49] L. Tomassetti,[17,a] D. Tonelli,[40] S. Topp-Joergensen,[57] F. Toriello,[61] E. Tournefier,[4] S. Tourneur,[41] K. Trabelsi,[41] M. Traill,[53] M. T. Tran,[41] M. Tresch,[42] A. Trisovic,[40] A. Tsaregorodtsev,[6] P. Tsopelas,[43] A. Tully,[49] N. Tuning,[43] A. Ukleja,[29] A. Ustyuzhanin,[35] U. Uwer,[12] C. Vacca,[16,k] V. Vagnoni,[15,40] A. Valassi,[40] S. Valat,[40] G. Valenti,[15] R. Vazquez Gomez,[19] P. Vazquez Regueiro,[39] S. Vecchi,[17] M. van Veghel,[43] J. J. Velthuis,[48] M. Veltri,[18,w] G. Veneziano,[57] A. Venkateswaran,[61] M. Vernet,[5] M. Vesterinen,[12] J. V. Viana Barbosa,[40] B. Viaud,[7] D. Vieira,[63] M. Vieites Diaz,[39] H. Viemann,[67] X. Vilasis-Cardona,[38,f] M. Vitti,[49] V. Volkov,[33] A. Vollhardt,[42] B. Voneki,[40] A. Vorobyev,[31] V. Vorobyev,[36,e] C. Voß,[9] J. A. de Vries,[43] C. Vázquez Sierra,[39] R. Waldi,[67] C. Wallace,[50] R. Wallace,[13] J. Walsh,[24] J. Wang,[61] D. R. Ward,[49] H. M. Wark,[54] N. K. Watson,[47] D. Websdale,[55] A. Weiden,[42] M. Whitehead,[40] J. Wicht,[50] G. Wilkinson,[57,40] M. Wilkinson,[61] M. Williams,[40] M. P. Williams,[47] M. Williams,[58] T. Williams,[47] F. F. Wilson,[51] J. Wimberley,[60] J. Wishahi,[10] W. Wislicki,[29] M. Witek,[27] G. Wormser,[7] S. A. Wotton,[49] K. Wraight,[53] K. Wyllie,[40] Y. Xie,[65] Z. Xing,[61] Z. Xu,[41] Z. Yang,[3] Y. Yao,[61] H. Yin,[65] J. Yu,[65] X. Yuan,[36,e] O. Yushchenko,[37] K. A. Zarebski,[47] M. Zavertyaev,[11,b] L. Zhang,[3] Y. Zhang,[7] Y. Zhang,[63] A. Zhelezov,[12] Y. Zheng,[63] X. Zhu,[3] V. Zhukov,[33] and S. Zucchelli[15]

(LHCb Collaboration)

[1]*Centro Brasileiro de Pesquisas Físicas (CBPF), Rio de Janeiro, Brazil*
[2]*Universidade Federal do Rio de Janeiro (UFRJ), Rio de Janeiro, Brazil*
[3]*Center for High Energy Physics, Tsinghua University, Beijing, China*
[4]*LAPP, Université Savoie Mont-Blanc, CNRS/IN2P3, Annecy-Le-Vieux, France*
[5]*Clermont Université, Université Blaise Pascal, CNRS/IN2P3, LPC, Clermont-Ferrand, France*
[6]*CPPM, Aix-Marseille Université, CNRS/IN2P3, Marseille, France*
[7]*LAL, Université Paris-Sud, CNRS/IN2P3, Orsay, France*
[8]*LPNHE, Université Pierre et Marie Curie, Université Paris Diderot, CNRS/IN2P3, Paris, France*
[9]*I. Physikalisches Institut, RWTH Aachen University, Aachen, Germany*
[10]*Fakultät Physik, Technische Universität Dortmund, Dortmund, Germany*
[11]*Max-Planck-Institut für Kernphysik (MPIK), Heidelberg, Germany*
[12]*Physikalisches Institut, Ruprecht-Karls-Universität Heidelberg, Heidelberg, Germany*
[13]*School of Physics, University College Dublin, Dublin, Ireland*
[14]*Sezione INFN di Bari, Bari, Italy*
[15]*Sezione INFN di Bologna, Bologna, Italy*
[16]*Sezione INFN di Cagliari, Cagliari, Italy*
[17]*Sezione INFN di Ferrara, Ferrara, Italy*
[18]*Sezione INFN di Firenze, Firenze, Italy*
[19]*Laboratori Nazionali dell'INFN di Frascati, Frascati, Italy*
[20]*Sezione INFN di Genova, Genova, Italy*
[21]*Sezione INFN di Milano Bicocca, Milano, Italy*
[22]*Sezione INFN di Milano, Milano, Italy*
[23]*Sezione INFN di Padova, Padova, Italy*
[24]*Sezione INFN di Pisa, Pisa, Italy*
[25]*Sezione INFN di Roma Tor Vergata, Roma, Italy*
[26]*Sezione INFN di Roma La Sapienza, Roma, Italy*
[27]*Henryk Niewodniczanski Institute of Nuclear Physics Polish Academy of Sciences, Kraków, Poland*
[28]*AGH - University of Science and Technology, Faculty of Physics and Applied Computer Science, Kraków, Poland*
[29]*National Center for Nuclear Research (NCBJ), Warsaw, Poland*
[30]*Horia Hulubei National Institute of Physics and Nuclear Engineering, Bucharest-Magurele, Romania*
[31]*Petersburg Nuclear Physics Institute (PNPI), Gatchina, Russia*
[32]*Institute of Theoretical and Experimental Physics (ITEP), Moscow, Russia*
[33]*Institute of Nuclear Physics, Moscow State University (SINP MSU), Moscow, Russia*
[34]*Institute for Nuclear Research of the Russian Academy of Sciences (INR RAN), Moscow, Russia*
[35]*Yandex School of Data Analysis, Moscow, Russia*
[36]*Budker Institute of Nuclear Physics (SB RAS), Novosibirsk, Russia*
[37]*Institute for High Energy Physics (IHEP), Protvino, Russia*
[38]*ICCUB, Universitat de Barcelona, Barcelona, Spain*

[39]Universidad de Santiago de Compostela, Santiago de Compostela, Spain
[40]European Organization for Nuclear Research (CERN), Geneva, Switzerland
[41]Institute of Physics, Ecole Polytechnique Fédérale de Lausanne (EPFL), Lausanne, Switzerland
[42]Physik-Institut, Universität Zürich, Zürich, Switzerland
[43]Nikhef National Institute for Subatomic Physics, Amsterdam, The Netherlands
[44]Nikhef National Institute for Subatomic Physics and VU University Amsterdam, Amsterdam, The Netherlands
[45]NSC Kharkiv Institute of Physics and Technology (NSC KIPT), Kharkiv, Ukraine
[46]Institute for Nuclear Research of the National Academy of Sciences (KINR), Kyiv, Ukraine
[47]University of Birmingham, Birmingham, United Kingdom
[48]H.H. Wills Physics Laboratory, University of Bristol, Bristol, United Kingdom
[49]Cavendish Laboratory, University of Cambridge, Cambridge, United Kingdom
[50]Department of Physics, University of Warwick, Coventry, United Kingdom
[51]STFC Rutherford Appleton Laboratory, Didcot, United Kingdom
[52]School of Physics and Astronomy, University of Edinburgh, Edinburgh, United Kingdom
[53]School of Physics and Astronomy, University of Glasgow, Glasgow, United Kingdom
[54]Oliver Lodge Laboratory, University of Liverpool, Liverpool, United Kingdom
[55]Imperial College London, London, United Kingdom
[56]School of Physics and Astronomy, University of Manchester, Manchester, United Kingdom
[57]Department of Physics, University of Oxford, Oxford, United Kingdom
[58]Massachusetts Institute of Technology, Cambridge, MA, United States
[59]University of Cincinnati, Cincinnati, OH, United States
[60]University of Maryland, College Park, MD, United States
[61]Syracuse University, Syracuse, NY, United States
[62]Pontifícia Universidade Católica do Rio de Janeiro (PUC-Rio), Rio de Janeiro, Brazil
(associated with Universidade Federal do Rio de Janeiro (UFRJ), Rio de Janeiro, Brazil)
[63]University of Chinese Academy of Sciences, Beijing, China
(associated with Center for High Energy Physics, Tsinghua University, Beijing, China)
[64]School of Physics and Technology, Wuhan University, Wuhan, China
(associated with Center for High Energy Physics, Tsinghua University, Beijing, China)
[65]Institute of Particle Physics, Central China Normal University, Wuhan, Hubei, China
(associated with Center for High Energy Physics, Tsinghua University, Beijing, China)
[66]Departamento de Fisica, Universidad Nacional de Colombia, Bogota, Colombia
(associated with LPNHE, Université Pierre et Marie Curie, Université Paris Diderot, CNRS/IN2P3, Paris, France)
[67]Institut für Physik, Universität Rostock, Rostock, Germany
(associated with Physikalisches Institut, Ruprecht-Karls-Universität Heidelberg, Heidelberg, Germany)
[68]National Research Centre Kurchatov Institute, Moscow, Russia
(associated with Institute of Theoretical and Experimental Physics (ITEP), Moscow, Russia)
[69]Instituto de Fisica Corpuscular (IFIC), Universitat de Valencia-CSIC, Valencia, Spain
(associated with ICCUB, Universitat de Barcelona, Barcelona, Spain)
[70]Van Swinderen Institute, University of Groningen, Groningen, The Netherlands
(associated with Nikhef National Institute for Subatomic Physics, Amsterdam, The Netherlands)

[a]Also at Università di Ferrara, Ferrara, Italy.
[b]Also at P.N. Lebedev Physical Institute, Russian Academy of Science (LPI RAS), Moscow, Russia.
[c]Also at Università di Milano Bicocca, Milano, Italy.
[d]Also at Università di Modena e Reggio Emilia, Modena, Italy.
[e]Also at Novosibirsk State University, Novosibirsk, Russia.
[f]Also at LIFAELS, La Salle, Universitat Ramon Llull, Barcelona, Spain.
[g]Also at Università di Bologna, Bologna, Italy.
[h]Also at Università di Roma Tor Vergata, Roma, Italy.
[i]Also at Università di Genova, Genova, Italy.
[j]Also at Scuola Normale Superiore, Pisa, Italy.
[k]Also at Università di Cagliari, Cagliari, Italy.
[l]Also at Università di Padova, Padova, Italy.
[m]Also at Università di Bari, Bari, Italy.
[n]Also at Laboratoire Leprince-Ringuet, Palaiseau, France.
[o]Also at Università degli Studi di Milano, Milano, Italy.
[p]Also at Universidade Federal do Triângulo Mineiro (UFTM), Uberaba-MG, Brazil.
[q]Also at AGH - University of Science and Technology, Faculty of Computer Science, Electronics and Telecommunications, Kraków, Poland.

[r]Also at Iligan Institute of Technology (IIT), Iligan, Philippines.
[s]Also at Hanoi University of Science, Hanoi, Vietnam.
[t]Also at Università di Pisa, Pisa, Italy.
[u]Also at Università di Roma La Sapienza, Roma, Italy.
[v]Also at Università della Basilicata, Potenza, Italy.
[w]Also at Università di Urbino, Urbino, Italy.